JOURNAL OF MATERIALS SCIENCE 29 (1994) 1250–1259

The influence of cell geometry on the elasticity of softwood

E. KAHLE
IRCAM, 31 rue Saint Merri, 75004 Paris, France
J. WOODHOUSE
Cambridge University Engineering Department, Trumpington Street, Cambridge, CB2 1PZ, UK

The cellular microstructure of softwoods such as spruce may be approximated as an irregular two-dimensional honeycomb. The nine macroscopic elastic constants of the wood, regarded as an orthotropic continuum, are governed by the geometric configuration of this honeycomb, together with the intrinsic material properties of the cell walls. Simple modelling is developed to allow all nine of these constants to be estimated from detailed microscopic measurements of the cell geometry, using assumed values for the cell-wall properties. Account is taken both of the cell-to-cell variations in growth and of the larger-scale modulation of cell properties in the annual growth rings. Results based on study of four samples of Norway spruce show very encouraging agreement with published measurements, and allow the relative importance of various effects to be assessed quantitatively.

1. Introduction

The cellular microstructure of wood makes it a member of the large family of foams and honeycombs. For all such materials, the macroscopic elastic constants are governed by the intrinsic elastic behaviour of the matrix material and by the geometric configuration of the microstructure [1]. To a large extent, these two factors can be studied separately. In this paper we investigate the contribution of the microstructure to the macroscopic elasticity of softwoods, taking the cell-wall elastic constants as parameters of the theory. Other studies give guidance on the possible values of these parameters, and on the origin of those values in the ultrastructure of the multi-layer composite of cellulose, hemicellulose and lignin which is the cell wall [2].

The main motivation for this study comes from the requirements of wood selection for the soundboards of musical instruments. The wood traditionally preferred for this purpose is Norway spruce (*Picea abies*), although certain other softwood species with generally similar properties are sometimes used. Makers of violins, guitars and so on are extremely particular about the choice, cut and seasoning of spruce for soundboards. One would like to understand their requirements in quantitative terms, so as to give guidance in the process of quality control. Also, as good spruce becomes scarce and thus expensive, one would like a basis for deciding which other materials, be they other wood species or man-made composites, might make possible alternatives.

Elastic constants are not the only quantities relevant to wood selection for musical instruments. Internal damping is also of great importance. Although nothing will be said explicitly about damping in this paper, it is hoped that the understanding of the micromechanics of deformation which comes from a study of elasticity could in future help the study of damping. After all, once one knows where the elastic strain energy is stored for a given macroscopic deformation, it is straightforward in principle to model the dissipation rate of that energy. But cell-wall damping properties are even less well-understood than cell-wall elastic properties, so a quantitative study of this nature is not yet possible.

One's first thought might be to approach the wood-selection problem by a programme of measurements. Surely it would be possible to measure relevant properties of a wide range of wood samples and compare the results with the expressed preferences of instrument makers? Some work of this nature has indeed been carried out [3, 4], but it is difficult to do this job thoroughly. The main problem is that even the simplest reasonable idealization of wood as an elastic continuum involves a large number of independent elastic constants to be measured. The three obvious principal directions in the tree have distinct properties. These directions are conventionally denoted L for longitudinal (vertical in the growing tree), R for radial and T for transverse (tangential to the annual rings in a horizontal plane). If we can ignore the curvature of the annual growth rings by imagining a large tree, then, at least approximately, the wood possesses a mirror symmetry in each of the planes LR, LT and RT. Since for a straight-growing tree these three planes are mutually perpendicular, this is an orthorhombic or orthotropic symmetry, and standard linear-elasticity theory tells us that there will be nine

0022–2461

independent elastic constants [5]. A typical choice for the purposes of description would be the three Young's moduli in the principal directions, E_L, E_R and E_T, the three shear moduli in the principal planes, G_{LR}, G_{LT} and G_{RT}, and three of the Poisson's ratios in the principal planes. We will use the notation ν_{LR} for the Poisson contraction in the R direction given a pure tensile stress in the L direction, and similarly for other combinations of directions. It is obvious that six Poisson's ratios of this kind may be defined, but they are not all independent. A standard reciprocal theorem [5] requires that, for example,

$$E_L \nu_{RL} = E_R \nu_{LR} \quad (1)$$

We thus have a set of nine parameters which are sufficient to characterize the linear elasticity of a given sample.

To measure values of all nine constants for a given wood sample is a difficult undertaking [6]. There are a few complete sets of data from the days when spruce was of interest in aircraft construction [7, 8], and there is some interesting recent work investigating the use of ultrasonic methods for all nine constants [9], but nearly all the published data gives only a restricted subset. Most often, only E_L, the long-grain stiffness, and E_R, the cross-grain stiffness, are quoted. (Instrument makers prefer wood cut in the LR plane, so-called *quarter-cut* wood, so the T direction runs normal to the surface of the finished soundboard.)

The hope behind the present study is that this daunting measurement task might be reduced if we understood how the values of the nine constants arise from the internal structure of the material. It is at least conceivable that the relevant variations in growth from tree to tree of a given species might not actually involve very many free parameters, so that the induced variations in the macroscopic elastic constants are correlated in some way of which we might take advantage. These underlying growth variations might affect the cell-wall elasticity or the cell geometry, but, in either case, to take advantage of any knowledge we would need to know how the cell-wall behaviour is linked to the macroscopic elasticity by the particular pattern of cell growth. Such understanding might also shed light on other questions, such as what influence on elastic behaviour should be expected from particular growth anomalies in a tree, or what effects might arise from changing the wood microstructure by, for example, permanent deformation by bending the wood to a desired shape.

The cellular structure of spruce is essentially quite simple [10]. The vast majority of the cells are *tracheids*, which run axially in the tree (in the L direction). They are needle shaped, with length-to-diameter ratios of the order of 15. The tracheids fit together to form an irregular honeycomb in the RT plane, whose properties are modulated in the radial direction by the annual growth rings. Spring growth produces large-diameter tracheids with thin walls, but as the growing season comes towards its close the cells become progressively smaller in radial extent and thicker-walled, until growth stops. The following season growth resumes, giving an abrupt change of structure to the large, thin-walled spring-wood cells. The only cells in spruce which do not run axially form the *rays*. Ray cells are less substantial than tracheids, and they are aligned radially, cutting across the honeycomb of tracheids. One ray consists of a stack of about ten cells, on top of each other in the L direction, and only a single cell thick in the T direction. In Norway spruce, ray cells make up only about 2% of the total. In the living tree these cells transport fluids, but in well-seasoned wood, as studied here, they are empty. The cell walls form a honeycomb structure whose properties give wood its special attributes, both desirable and undesirable, as a material.

Efforts to model this cellular structure to find its influence on the elastic properties go back to Price [11], who approximated the tracheid honeycomb by a close-packed array of circular tubes. This allowed him to explain immediately the very high anisotropy between E_L and E_R or E_T. To stretch the wood in the L direction requires extension in the cell walls, but a stretch in the R or T directions can be achieved by bending the walls without extension. Since they are thin, the associated macroscopic stiffness is much lower. More recently, Ashby and Gibson [12] obtained similar results from a rather more accurate model, in which the tracheids were represented by a two-dimensional honeycomb whose cross-section takes the form of a regular array of hexagons.

The aim of the present study is to proceed one step beyond these previous investigations, by taking some account of the non-uniformity of the cell structure. This term covers the cell-by-cell variations of growth, and also the systematic modulation of properties consequent on the annual ring structure. An effort has been made to calculate all nine of the elastic constants for four spruce samples, based on a detailed study of the microstructure. Values for the cell-wall elastic constants have been taken from the literature, but in some cases we will argue that these values may not be accurate, at least for our samples.

One specific issue to be examined is the source of anisotropy between E_R and E_T. Typical measured values suggest that E_R/E_T is about 1.7 [7, 8]. Three different effects can be identified which contribute to this anisotropy, and we shall try to assess their relative importance. All three have been mentioned in previous literature. First, Price [11] considered the role of the annual rings. It is intuitively clear that the relatively dense, stiff layers of summer wood will reduce the ratio E_R: E_T and, if this were the only factor, would make this ratio *lower* than unity. Compression can occur in the R direction by bending only thin cell walls of the spring wood, but to achieve compression in the T direction the summer wood and spring wood must both be compressed. Put another way, the different properties of the spring wood and summer wood appear in series for R-direction deformation, but in parallel for T-direction deformation. Thus different averages must be taken in the two cases, leading to different macroscopic stiffnesses.

Clearly some other effect must compensate for this one, since it operates in the wrong direction. One such effect is the role of ray cells. Barkas [13] pointed out

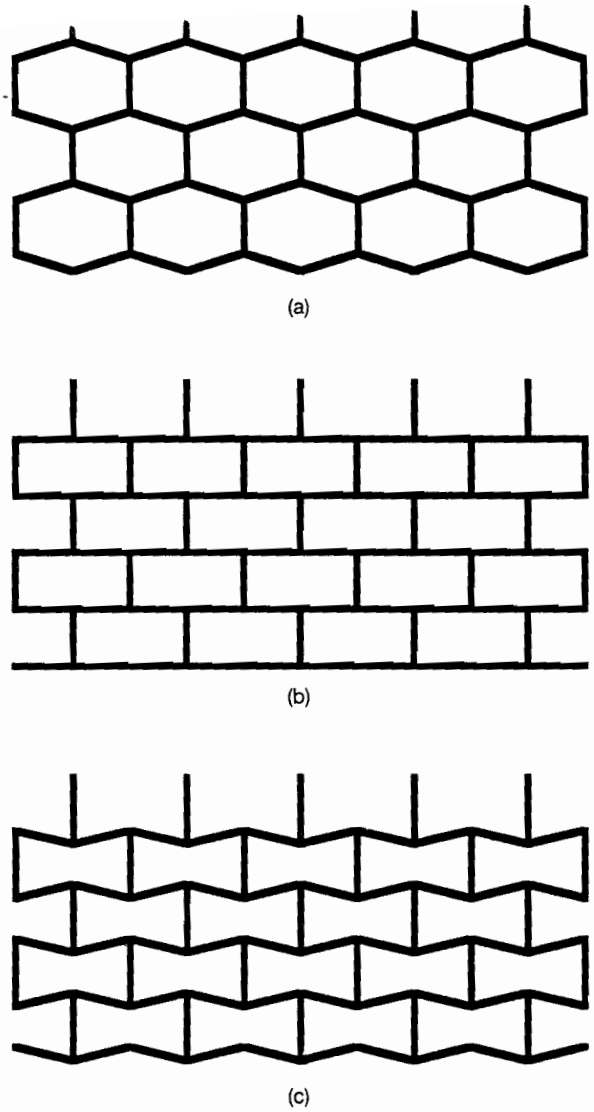

Figure 1 Three typical configurations of hexagonal honeycomb as analysed by Ashby and Gibson [1, 12, 14].

that the radial ray cells will contribute additional stiffness in the R direction, with negligible influence on the T direction. The mechanism is essentially the same as that outlined above for the $E_L:E_R$ anisotropy. The third influence on $E_R:E_T$ is the effect of cell geometry in the RT plane, as discussed by Ashby and Gibson [1, 12]. Their theory treated any regular tesselation of hexagons, some examples being illustrated in Fig. 1. Most of these configurations will lead to anisotropy in the RT plane, the most extreme case being shown in Fig. 1b. Here, it is possible to compress the material in one direction by cell-wall bending, but the walls are all aligned in the other direction so that macroscopic compression can only be achieved by local cell-wall compression. Obviously, a large anisotropy of Young's modulus will result.

2. Determination of the elastic constants

2.1. Preliminaries

The cell wall is itself an anisotropic material, built up as a multi-layered composite of cellulose, hemicellulose and lignin [2, 10]. It should be noted that when we refer here to *a cell wall*, we mean one structural unit of the model as an irregular honeycomb. This unit actually consists of the walls of two adjacent cells, together with the layer of lignin holding them together. This symmetric back-to-back structure makes it reasonable to assume that the whole unit is two-dimensionally orthotropic, so that its in-plane elastic properties may be specified by four elastic constants: two Young's moduli, one in-plane Poisson's ratio and the in-plane shear modulus. When treating the very thick-walled summer-wood cells, the Poisson's ratios relating to contraction through the thickness of the wall resulting from in-plane extension will also play a small role in the results.

Values for all these elastic constants can be found in the literature, although some values are much more certain than others. To distinguish cell-wall constants from macroscopic constants for the wood, lower case letters will be used to indicate directions; thus E_l will denote the longitudinal Young's modulus of the cell wall, E_t the transverse Young's modulus (which of course might be oriented anywhere in the RT plane in the wood), G_{lt} the in-plane shear modulus, ν_{lt} the transverse Poisson contraction given an axial stretch, and (somewhat inconsistently) ν_{tr} the Poisson contraction through the thickness of the wall given a transverse in-plane stretch. Typical values cited for these constants, together with the density ρ_s of the solid cell-wall substance, are given in Table I. (*Staypak* is a material made by compressing wood under high temperature and pressure, which has a final density nearly as high as the value cited for the cell-wall substance. It gives the only direct measurements available for Poisson's ratios.) Table I also gives suggested alternative values for some of the cell-wall constants based on this study; these values will be discussed in Section 3.

We shall make extensive use of the honeycomb model of Ashby and Gibson, and of extensions to it using similar approximations of simple beam theory. It is useful to begin by summarizing the main results. For a unit cell, the necessary geometric notation is defined in Fig. 2a. The expressions given by Ashby *et al.* for the in-plane elastic constants are

$$
\begin{aligned}
E_x &= \frac{E_m d^3 \cos\theta}{w^3(h/w + \sin\theta)\sin^2\theta}, \\
E_y &= \frac{E_m d^3(h/w + \sin\theta)}{w^3\cos^3\theta} \\
\nu_{xy} &= \frac{\cos^2\theta}{(h/w + \sin\theta)\sin\theta}, \\
\nu_{yx} &= \frac{(h/w + \sin\theta)\sin\theta}{\cos^2\theta} \\
G_{xy} &= \frac{E_m d^3(h/w + \sin\theta)}{w^3(h/w)^2(2h/w + 1)\cos\theta}
\end{aligned}
\tag{2}
$$

These equations assume a matrix with a Young's modulus E_m, and a deformation involving bending only (with no compression or shear). The coordinate directions are labelled x and y. These will correspond,

TABLE I Values of cell-wall properties from the literature

Property	Value from literature	Source	Suggested value
ρ_s	1500 kg m^{-3}	[16], [2]	1500 kg m^{-3}
E_l	35 GPa	[15]	40–50 GPa
E_t	10 GPa	[15]	9 GPa
G_{lt}	2.6 GPa	[1]	3.5–4 GPa
ν_{lt}	0.4	[2] (from Staypak)	0.5
ν_{tl}	0.15	[2] (from Staypak)	0.1
ν_{tr}	0.6	[2] (from Staypak)	0.6

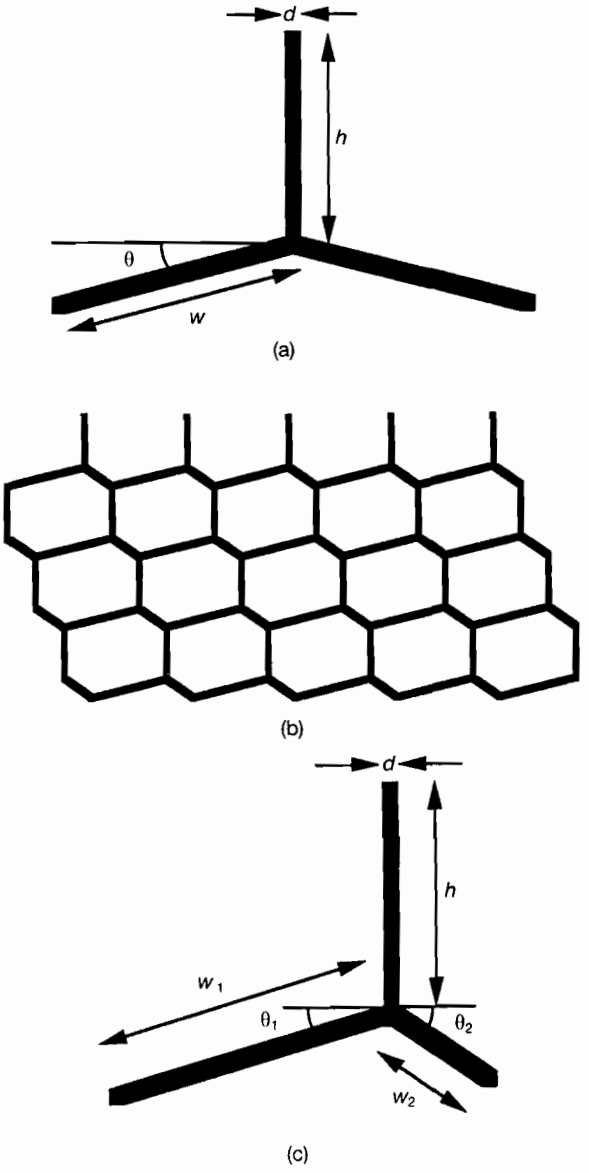

Figure 2(a) One structural unit of a honeycomb of the type shown in Fig. 1, with definitions of some geometric notation; (b) an example of a periodic honeycomb built from irregular hexagonal cells; (c) one structural unit of the honeycomb shown in (b), with the geometric parameters marked.

broadly, to the directions R and T, respectively. Gibson [14] has also described extensions of this theory to allow for compression and shear. A typical result, which will be of direct interest to us, as will be seen in the next subsection, is

$$E_x = \frac{E_m d^3 \cos\theta}{w^3(h/w + \sin\theta)\sin^2\theta[1 + (2.4 + 1.5\nu_m + \cot^2\theta)(d/w)^2]} \quad (3)$$

where ν_m is the matrix-material Poisson's ratio. Here, the term involving $2.4 + 1.5\nu_m$ allows for shear, while the term involving $\cot^2\theta$ allows for compression.

The first step in using this theory for actual wood structures is to extend it to regular tesselations of non-symmetric hexagons. Fig. 2b shows a typical example, and Fig. 2c shows one unit from which the whole pattern may be built by repetition. Some further geometric notation is also defined in Fig. 2. Our procedure, at least for the analysis in the RT plane, will be to represent the cell structure by a number of three-pronged elements as shown in Fig. 2c, each with its own values of the geometric parameters.

The investigation begins with scanning electron micrographs of the cell structure, sectioned in the RT plane. Two examples are shown in Fig. 3a and b, one from the spring wood, the other showing the summer wood and the sharp transition between two seasons' growth. Several rays can be seen crossing the micrographs horizontally. The spruce for the investigation

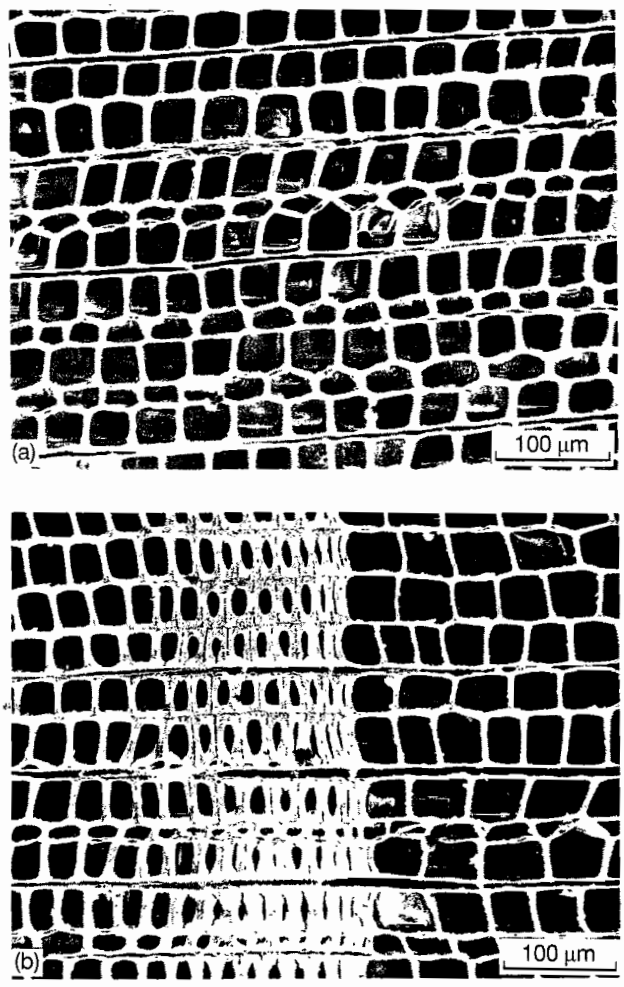

Figure 3 Scanning electron micrographs of the RT plane in one of the samples of Norway spruce analysed in this study: (a) early-spring growth; (b) the transition through the summer growth of one annual ring. The T direction runs parallel to the annual ring and the R direction runs approximately horizontally, the growth direction of the tree being from left to right.

was obtained from a violin-maker's workshop, so that all the samples were straight grained, knot-free and well-seasoned. For each sample, a montage of micrographs was prepared which allowed detailed analysis to be carried out for a strip which was one complete annual ring in radial extent and 15 cells wide in the T direction. These strips each contained 500–700 cells.

The geometric parameters for each three-pronged element within the analysed strips were measured from the micrographs, and entered into a computer to facilitate the processing required. The Ashby/Gibson theory can be used to predict the elastic properties of each element, then appropriate averaging procedures can be applied to aggregate the results into macroscopic elastic constants. The objective is not to model the behaviour of the irregular structure with complete accuracy, but to use approximations which capture the main effects so that their influence may be assessed.

2.2. The Young's moduli

We first discuss the Young's moduli in the three principal directions. The easiest to calculate, within the simple theory in use here, is E_L. For this, we need only find the fraction of the cross-sectional area in the micrographs which is occupied by wood substance rather than empty space. The value of E_L is then the cell-wall modulus E_1 multiplied by this fraction, since the assumption is that axial loads are carried by compressive force in all the tracheid tubes. Equivalently, we may multiply E_1 by the relative density of the wood compared with that of wood substance, provided we neglect the ray cells which will contribute to the mass but not to the axial load-bearing capacity.

To obtain the other two Young's moduli, E_R and E_T, requires more work. It is immediately clear from Fig. 3 that the two cases are rather different. There is a strong degree of cell alignment in the R direction, whereas the cells are randomly staggered in the T direction. This is a consequence of the normal pattern of tree growth, in which each tracheid in the outermost layer divides to produce another alongside it, forming a new outer layer. It is reasonable to suppose that a load in the R direction will be carried along zig-zag lines like the one labelled R line in Fig. 4, which is a diagrammatic version of Fig. 3a. In each line, the deformation will involve a combination of bending and compression in the segments of the zig-zag. The sections of cell wall oriented in the T direction will contribute very little to the overall stiffness, and they will be ignored in the calculation. When we come to calculate E_T, on the other hand, a rather more artificial concept of the T lines is needed. An example is indicated in Fig. 4. It is made up of a column of three-pronged elements, each analogous to Fig. 2c. A load in the T direction will be carried through the set of such columns, by a combination of bending in the cell walls which form part of the R lines, and compression in the other walls.

For both cases, the same general procedure may be followed. The lines are assumed to be free to move independently. Any relative motion between adjacent

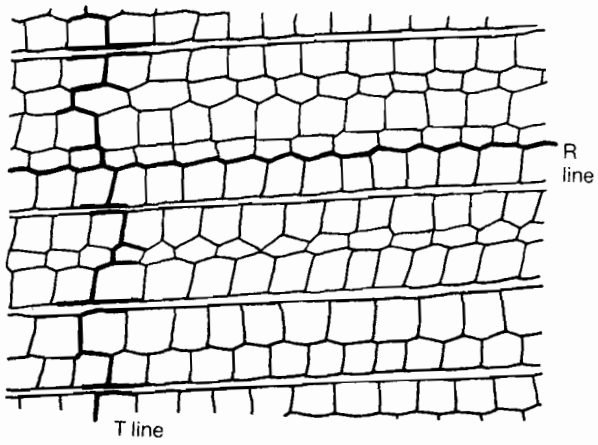

Figure 4 A diagrammatic version of Fig. 3a, showing a typical T line and a typical R line, as described in the text.

lines will be accommodated by bending and shear deformation in the cross-links, but we expect this to contribute very little to the overall stiffness, since in both cases adjacent lines are generally sufficiently similar that such relative motion will be quite slight. We now imagine the whole sample under a uniaxial load in the relevant direction. Each line will carry a fraction of the applied load, which will be constant along the line; the motion of each element will adjust itself according to its own stiffness. The distribution of force between the different lines, though, is governed by a condition of equal *displacement*, if we imagine a test in which the sample is compressed between flat, rigid platens. Thus an appropriate way to combine the stiffnesses of the individual three-pronged elements is a combination of a series connection (along the lines) and a parallel connection (between lines).

This procedure is readily carried through, using the measured data on each element in a given sample. It transpires that the strong alignment of cell walls in the R direction leads to a considerable fraction of the load in that direction being carried by compression rather than bending. The corrected formula (3) is thus essential to obtain sensible results for this case, although the allowance for shear also included in this formula has only a small effect, and can be omitted. In the T direction there is also some effect of compression (in the walls running vertically in Fig. 2), but the overall stiffness is governed primarily by bending in the other walls, so that no great error is made by omitting it.

Note that the effect of rays is automatically included in the analysis just described, at least up to a point. Where a ray cell is visible in a micrograph, its wall thickness and influence on cell alignment is included in the measurements of individual structural elements. The only error as a consequence of this is that we use the transverse material properties of tracheid walls in calculating stiffnesses from the geometric measurements, whereas we should use the (presumably different) axial material properties of ray-cell walls. But the number of rays in spruce is so small in relation to the number of tracheids that only a very small error will result in the macroscopic predictions.

There is one further issue to be considered in relation to E_R and E_T, which is whether the simple procedure

just described copes adequately with the thicker-walled cells of the summer wood. The relative density there is often around 0.5, which is more suggestive of a solid material with inclusions than of a structure of thin beams. The implications of this raise rather separate issues for E_R and E_T. When calculating E_R, we should consider the role of Poisson's ratio, which varies significantly across an annual ring. This will be addressed in detail in the next subsection.

When the simple theory is applied to calculate E_T, a single line in the summer-wood area is predicted to be some 10–20 times stiffer than a line in the spring-wood area, and the summer wood contributes up to 80–90% of the total stiffness. This makes it imperative to treat this area carefully, and not to rely on inappropriate approximations chosen because they work well enough for the spring wood. A particular problem concerns the estimation of the cell-wall thickness in the summer wood. Careful examination of micrographs reveals that the wall thickness is quite variable in this area (a variation by a factor of two within one wall has been observed), and that defects such as cracks and voids are quite common (perhaps as a result of the drying during seasoning of the wood). When such a high proportion of the load is carried by this area of the structure, any such *weak links* in the chain of transmission could produce a very significant reduction in the overall stiffness.

For the purposes of this study, it was decided to allow for such effects by the rather crude method of assigning an *equivalent thickness* to the cell walls in the summer-wood area when calculating stiffnesses. The value chosen for this in the sample shown in Fig. 3 was 4.5 μm, compared with 3.1 μm measured in the early-spring wood, and 3.6 μm in the later-spring wood. Some support for this approach, and for the values chosen, has been obtained by two methods. First, the pattern of deformation was observed when the summer wood was deformed dynamically inside a scanning electron microscope, and the important role of weak links was then evident. Secondly, the calculations to be described in the next section give independent estimates of E_R, E_T, ν_{RT} and ν_{TR}, which depend on this choice of equivalent thickness. The reciprocal relation between the four quantities then gives a check on the self-consistency of the modelling.

2.3. The RT-plane Poisson's ratios

Of the two RT-plane Poisson's ratios, ν_{TR} is easier to estimate than ν_{RT}. When the Ashby/Gibson theory, suitably corrected for compression effects [14], is applied to regular honeycombs based on the individual three-pronged elements of the spruce structure, wide variations in Poisson's ratio across the annual ring are predicted. In the early-spring wood, values approaching or even exceeding unity are found for ν_{RT}. (Recall that in a two-dimensional structure there are no theoretical constraints on the value of Poisson's ratio, and any positive or negative value is possible in principle.) In the late-spring wood, values around 0.5 are common, while, in the summer wood, values as low as 0.2 are found. These last values are probably rather too low – the measurements on Staypak given in Table I indicate that solid-wood substances have a Poisson's ratio of around 0.6 in the transverse plane. As has already been noted, summer wood approaches the condition of being a solid with small inclusions, so the value from the Ashby/Gibson theory should probably be increased. We will return to this question in Section 3, when numerical results are discussed.

In any case, the variations across the annual ring must be allowed for. If we imagine a uniform compressive strain imposed in the T direction, these variations do not cause any problem. Each layer of cells (parallel to the rings) has an approximately uniform structure, so they will exhibit a Poisson expansion governed by the local properties. The overall expansion is simply the sum of the expansions in each layer, so that a reasonable estimate of ν_{TR} should be obtained by a simple average.

Things are different when we took at ν_{RT}. The long-range constraints exerted by the annual-ring structure must be allowed for in combining the individual values to give a macroscopic result. When a strain is imposed in the R direction, the different layers will expand in the T direction by different amounts, and the compromise which results must be calculated by a different style of argument from that used so far. Of course, we could simply use the reciprocal relation to evaluate ν_{RT}, given that we already have estimates of ν_{TR}, E_R and E_T. But it is instructive, and a useful check on the other calculations, to find a way to make a direct estimate of ν_{RT}.

A simple approach to this problem utilises the variational principle for elasticity. We may model an annual ring adequately for this purpose by a structure with several discrete layers, each being assumed uniform in its properties. We may then impose a specified total strain in the R direction, and calculate that strain in the T direction which minimizes the total strain energy. This calculation will also improve the estimate of E_R discussed in the previous subsection, since it too is influenced by the constraining effect of the layer of dense summer wood. We have chosen to use a three-layer model, corresponding to the early-spring wood, late-spring wood, and summer wood. Of course, the boundaries between these regions are not sharp in most cases but the approximation seems to produce reasonable results.

Consider first a homogeneous, two-dimensional, orthotropic material with principal axes in directions which we may label x and y. It will have Young's moduli E_x and E_y, and Poisson's ratios ν_{xy} and ν_{yx}. For a deformation involving strains ε_x and ε_y along the principal directions, with no shear, the strain energy density is [8]

$$V = \frac{E_x\varepsilon_x^2 + E_y\varepsilon_y^2 + 2\nu_{yx}E_x\varepsilon_x\varepsilon_y}{2\mu} \qquad (4)$$

where $\mu = 1 - \nu_{xy}\nu_{yx}$. This may be readily extended to the three-layer model shown in Fig. 5, in which the properties in the three regions are distinguished by superscripts (1), (2) and (3), respectively. The lengths of the regions, $a^{(1)}$, $a^{(2)}$ and $a^{(3)}$, are specified as fractions of the total length, so that $a^{(1)} + a^{(2)} + a^{(3)} = 1$. We

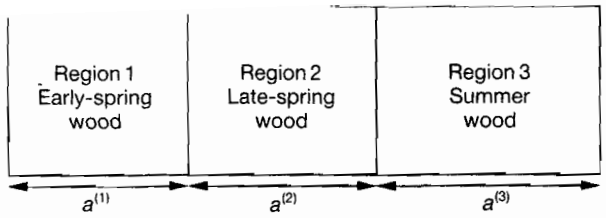

Figure 5 The three-layer model used to analyse the constraining effect of the annual ring on motion in the RT plane. The total width covers one annual ring.

can impose a total strain ε_x. We do not know *a priori* how this is partitioned into the strains $\varepsilon_x^{(1)}$, $\varepsilon_x^{(2)}$ and $\varepsilon_x^{(3)}$ in the separate regions, but we must have

$$a^{(1)}\varepsilon_x^{(1)} + a^{(2)}\varepsilon_x^{(2)} + a^{(3)}\varepsilon_x^{(3)} = \varepsilon_x \quad (5)$$

Since we are considering deformation in the interior of a large specimen (compared with the ring spacing), the transverse strain, ε_y, resulting from Poisson's-ratio effects must be the same in all regions. So the total strain-energy density is

$$V = \frac{E_x^{(1)}\varepsilon_x^{(1)2} + E_y^{(1)}\varepsilon_y^{(1)2} + 2\nu_{yx}^{(1)}E_x^{(1)}\varepsilon_x^{(1)}\varepsilon_y^{(1)}}{2\mu^{(1)}} + \frac{E_x^{(2)}\varepsilon_x^{(2)2} + E_y^{(2)}\varepsilon_y^{(2)2} + 2\nu_{yx}^{(2)}E_x^{(2)}\varepsilon_x^{(2)}\varepsilon_y^{(2)}}{2\mu^{(2)}} + \frac{E_x^{(3)}\varepsilon_x^{(3)2} + E_y^{(3)}\varepsilon_y^{(3)2} + 2\nu_{yx}^{(3)}E_x^{(3)}\varepsilon_x^{(3)}\varepsilon_y^{(3)}}{2\mu^{(3)}} \quad (6)$$

This must be minimized with respect to $\varepsilon_x^{(1)}$, $\varepsilon_x^{(2)}$, $\varepsilon_x^{(3)}$ and ε_y, subject to the constraint of Equation 5. In terms of a Lagrange multiplier, λ, we require that

$$\frac{\partial}{\partial\varepsilon_x^{(1)}}[V + \lambda(a^{(1)}\varepsilon_x^{(1)} + a^{(2)}\varepsilon_x^{(2)} + a^{(3)}\varepsilon_x^{(3)})] = 0 \quad (7)$$

$$\frac{\partial}{\partial\varepsilon_x^{(2)}}[V + \lambda(a^{(1)}\varepsilon_x^{(1)} + a^{(2)}\varepsilon_x^{(2)} + a^{(3)}\varepsilon_x^{(3)})] = 0 \quad (8)$$

$$\frac{\partial}{\partial\varepsilon_x^{(3)}}[V + \lambda(a^{(1)}\varepsilon_x^{(1)} + a^{(2)}\varepsilon_x^{(2)} + a^{(3)}\varepsilon_x^{(3)})] = 0 \quad (9)$$

and

$$\frac{\partial}{\partial\varepsilon_y}[V + \lambda(a^{(1)}\varepsilon_x^{(1)} + a^{(2)}\varepsilon_x^{(2)} + a^{(3)}\varepsilon_x^{(3)})] = 0 \quad (10)$$

These equations together with the constraint of Equation 5 give a set of five linear equations from which λ may be eliminated, and which may then be solved for $\varepsilon_x^{(1)}$, $\varepsilon_x^{(2)}$, $\varepsilon_x^{(3)}$ and ε_y in terms of the specified ε_x. The algebraic expressions are not worth displaying, but numerical results will be given in Section 3. The desired Poisson's ratio is now given by

$$\nu_{RT} = -\varepsilon_y/\varepsilon_x \quad (11)$$

since we have identified the directions in the following way: $x = R$, $y = T$. If the results are substituted back into the strain energy density Equation 6, so that it takes the form

$$V = \tfrac{1}{2}E^*\varepsilon_x^2 \quad (12)$$

then the coefficient E^* is an improved estimate for E_R.

2.4. The shear moduli

The final elastic constant relating to the RT plane is the shear modulus G_{RT}. This is governed by cell-wall bending to a very good approximation, and no correction for shear or compression need be employed in calculating the shear stiffness of each individual element in the structure. To aggregate these into a macroscopic shear modulus involves a similar procedure to that employed for the Young's moduli. We may imagine imposing a shear deformation between two platens which lie parallel to the LR plane and which are moved relative to one another along the R axis. It seems reasonable to suppose that the strong alignment of cell walls in the R direction produces something approaching a constant-displacement constraint along each R line. So the individual values of shear stiffness of the cell units along each R line should be combined by a simple arithmetic mean, then the lines are combined by a harmonic mean.

The other two shear moduli depend on the shear modulus of the cell-wall material. If a shear deformation is imposed in, for example, the LR plane, this will be resisted primarily by shear deformation in the cell walls aligned roughly in the R direction. The precise three-dimensional pattern of response will also no doubt involve some cell-wall bending, but the stiffness for bending is so much smaller than for in-plane shearing that one would expect it to contribute negligibly to the macroscopic shear modulus. To produce simple estimates for G_{LR} and G_{LT}, we will assume a rectangular geometry for the honeycomb of tracheids. This would be stiffer than the actual structure, with its staggered cells, so that we will overestimate the shear modulus (for a given assumed value of the cell-wall shear modulus). But it is hard to see how else to proceed, since there is no theory for the three-dimensional deformation of a honeycomb as simple as that which was used earlier in two dimensions (see the discussion (in section 4.5) by Gibson and Ashby [1]). With this assumption, it is simple to produce estimates for the shear stiffness of individual cells for shear in the LR and LT planes. These could be aggregated in the same manner described above for G_{RT}, but since we are calculating an upper bound based on rather crude modelling, a simple average of individual values seems equally valid within the expected limits of accuracy.

2.5. The remaining Poisson's ratios

Finally, we consider the Poisson's ratios which involve the L direction. For an imposed compressive strain in the L direction, the simple model we are using predicts that the Poisson expansions in the R and T directions will be simply that of a solid-wood substance, ν_{lt}. It makes no difference that the structure has axial holes in it, since each cell wall will expand by the same

factor, and the entire honeycomb pattern expands without distortion. The only exception to this argument, within the approximations we have used throughout, comes from the ray cells. These will provide a small degree of additional stiffening of the R direction, and perhaps reduce the Poisson expansion in that direction. But, in any case, the value for the cell-wall Poisson's ratio is quite uncertain, and it is far from clear that all cells should be assigned the same value. The thicker walls of the summer-wood cells might well have a different detailed structure of layers and winding angles, but there is insufficient data available to incorporate any such effects in theoretical models. By comparison with this uncertainty, the effect of stiffening by rays is probably quite minor for spruce (with its very small proportion of ray cells).

When a compressive strain is imposed in the R or T direction, a slightly different argument is needed. Bending of cell walls in the RT plane produces no strain in the L direction. The Poisson expansion is associated entirely with the compressive component of deformation in the RT plane, via the Poisson's ratio ν_{tl} of the cell wall. The cell-wall compression has already been calculated, in the course of estimating E_R and E_T. An average over all cells of the respective Poisson expansions implied by this argument yields macroscopic estimates of ν_{RL} and ν_{TL}.

3. Numerical results and discussion

When the estimation methods just described are applied, using the first set of cell-wall properties given in Table I, the results for the spruce sample illustrated in Fig. 3 (sample 1) are as listed in Table II under the heading First estimate. We will discuss these results in relation to the values expected from earlier measurements, and the comparison will lead us to suggest modifications to the cell-wall properties. These modified values are then applied to all four spruce samples analysed, the results are shown in Table II. It would have been desirable to measure the elastic properties of the actual spruce samples studied here, but that was unfortunately not possible. So the predicted values are compared with results given by Carrington [7]. He gives values for five samples, and we reproduce one typical set and the range for each constant in Table II.

We now compare the first-estimate values with Carrington's results in Table II. First, we see that the predicted value of E_L is rather low. Within the theory used here, there is a direct proportionality between E_L and the density, and we have a value of density which lies well within Carrington's range. We conclude that the factor of proportionality, which is governed by the cell-wall axial modulus, E_l, must be too small. The value 35 GPa for E_l in Table I was given by Cave [15] and it has been adopted by numerous subsequent authors. But if we look at the relationship between density and E_L in Carrington's data, we conclude that a better value for E_l lies in the range 40–50 GPa.

The predicted values of E_R and E_T are within Carrington's range, although they are a little on the high side. A slightly reduced value for the cell-wall transverse modulus, E_t, of 9 GPa gives a better fit, and we tentatively suggest this value for our samples. The value of E_R is based on the three-layer model described in Section 2.3, which deserves a little more comment. For the spruce sample studied here, the averaged parameters determined for the three layers using the Ashby/Gibson theory are listed in Table III. It has

TABLE II Predicted and measured elastic constants and density for spruce

Constant	First estimate	Typical results (Carrington [7])	Range	Best estimates			
				Sample 1	Sample 2	Sample 3	Sample 4
ρ (kg m^{-3})	400	430	370–500	400	400	430	440
E_L (GPa)	9.3	13.5	9.9–16.6	12.0	11.9	12.9	13.2
E_R (GPa)	0.91	0.89	0.64–0.89	0.79	0.74	0.71	0.82
E_T (GPa)	0.56	0.48	0.39–0.69	0.50	0.46	0.53	0.69
G_{RT} (GPa)	0.027	0.032	0.022–0.037	0.027	0.029	0.050	0.042
G_{RL} (GPa)	1.01	0.72	0.50–0.72	0.58	0.61	0.66	0.61
G_{TL} (GPa)	1.03	0.50	0.50–0.84	0.59	0.60	0.66	0.70
ν_{RT}	0.32	0.56	0.43–0.64	0.44	0.51	0.51	0.43
ν_{TR}	0.30	0.30	0.25–0.33	0.29	0.29	0.30	0.27
ν_{RL}	0.057	0.030	0.018–0.031	0.028	0.030	0.024	0.035
ν_{LR}	0.4	0.45	0.36–0.45	0.4	0.4	0.4	0.4
ν_{TL}	0.047	0.019	0.013–0.023	0.019	0.019	0.013	0.027
ν_{LT}	0.4	0.54	0.38–0.56	0.4	0.4	0.4	0.4

TABLE III Parameters for the three-layer model

Region	Length proportion, a	E_R/E_t	E_T/E_t	ν_{RT}	ν_{TR}	μ
1: early-spring wood	0.58	0.072	0.018	0.772	0.269	0.83
2: late-spring wood	0.30	0.098	0.044	0.529	0.231	0.85
3: summer wood	0.12	0.163	0.274	0.091	0.165	0.97

already been noted that the Poisson's ratio for the summer wood (region 3) is probably too low, so the influence of this Poisson's ratio on the predicted macroscopic results was investigated. One useful indicator is the accuracy with which the reciprocal relation

$$E_R \nu_{TR} = E_T \nu_{RT} \quad (13)$$

is satisfied. We may evaluate both sides of this equation with any assumed value of $\nu_{RT}^{(3)}$ for the summer wood, with results as given in Table IV. This suggests that we use a value of around 0.5 for $\nu_{RT}^{(3)}$ in the summer-wood area, which is quite in keeping with the measured value from Staypak given in Table I.

The other anomalies to note in this first comparison between theory and measurements concern the shear moduli and Poisson's ratios which involve the L direction. As was explained in Sections 2.4 and 2.5, these are heavily dependent on cell-wall properties for which reliable measurements do not exist. The values from the literature given in Table I were determined by data fits to macroscopic behaviour, and there is no reason to believe them to be more accurate than the calculations carried out here. We thus suggest that our modelling be used to give amended values for those properties, at least for our spruce samples. The suggested values are given in the last column of Table I.

Using the set of cell-wall properties as amended by the first comparison, the full set of elastic constants for the four spruce samples studied are given in the four final columns of Table II. The level of agreement with Carrington's data now seems entirely satisfactory.

One aspect of the results remains to be discussed. In Section 1, we discussed three possible sources of anisotropy between E_T and E_R. Now that we have models for both constants which reproduce that anisotropy with reasonable accuracy, we can use them to examine the three effects which have been suggested to account for it. At least for our particular samples, the answer is as follows. The annual-ring structure has an influence of the kind described, tending to make $E_T > E_R$. The summer wood accounts for some 50% of the T-direction stiffness, while occupying only 10–15% of the area. (Of course, wood with different growth patterns might show quite different results.)

The effect of rays is rather different in detail from the description advanced by Barkas [13]. The rays do indeed have an effect of additional stiffening in the R direction, but not so much from the radial alignment of their own walls as from the alignment they induce in the walls of the neighbouring tracheids. In general, an R line containing a ray is about 50–100% stiffer than a "normal" line. Since the two sides of a ray which is intersected in the analysed section contribute separate lines, the net effect is that putting a ray between two rows of tracheids yields a combined stiffness three or four times higher than the zig-zag line without the ray. Given the typical spacing of rays in our specimens, we can say that perhaps 25–50% of the radial stiffness is due to rays in this sense. This is of about the same order of magnitude as the effect of annual rings in stiffening the T direction – the two effects approximately cancel one another out in these particular samples.

The third effect, from the geometry of the honeycomb, is therefore of about the right magnitude to provide the observed anisotropy, of rather less than a factor of two. In detail, it turns out that in the spring wood a typical R line is some 3–5 times stiffer than a typical T line, but the local anisotropy decreases through the late-spring wood into the summer wood, the aggregate values giving the observed effect.

TABLE IV The effect of varying $\nu_{RT}^{(3)}$

$\nu_{RT}^{(3)}$	E_R/E_t	E_T/E_t	ν_{RT}	ν_{TR}	$\nu_{TR}E_R/E_t$	$\nu_{RT}E_T/E_t$
0.1	0.091	0.056	0.32	0.25	0.023	0.018
0.5	0.087	0.056	0.44	0.29	0.025	0.025
0.8	0.086	0.056	0.52	0.32	0.028	0.029

4. Conclusions

Simple predictive models have been constructed for all the elastic constants of spruce, regarded on a macroscopic scale as an orthotropic (orthorhombic) continuum. At the cellular level, spruce is modelled as an irregular honeycomb of tubes. The actual geometry was measured for samples of 500–700 individual cells in four separate specimens of Norway spruce. Local elastic properties were deduced from the geometry of each structural element, and suitable procedures were devised for aggregating these into macroscopic elastic constants. In some cases these were simple averaging procedures, but in others the long-range constraining effect of the annual-ring structure was allowed for by a variational calculation. The results were compared with published measurements of the elastic constants of spruce, and it was argued that the only significant anomalies might result from inadequacies in the data on the cell-wall properties. Revised values have been suggested for certain of these properties, for our particular samples, and when these were used very satisfactory agreement was achieved between the predictions for all four samples and the previous measurements.

Acknowledgements

The authors express their gratitude to Dr C. Y. Barlow for the electron micrographs used in this study, and to her and Professor M. F. Ashby for many helpful discussions.

References

1. L. J. GIBSON and M. F. ASHBY, "Cellular solids" (Pergamon, Oxford, 1988).
2. R. E. MARK, "Cell wall mechanics of tracheids" (Yale University Press, 1967).
3. J. C. SCHELLENG, *Catgut Acoust. Soc. Newsletter* **37** (1982) 8.
4. D. W. HAINES, *ibid.* **31** (1979) 23.
5. R. F. S. HEARMON, "Introduction to applied anisotropic elasticity" (Oxford University Press 1961).
6. M. E. MCINTYRE and J. WOODHOUSE, *Acta Metall.* **36** (1988) 1397.

7. H. CARRINGTON, *Phil. Mag.* **45** (1923) 1055.
8. R. F. S. HEARMON, "The elasticity of wood and plywood" (Forest Products Research Special Report No. 7, His Majesty's Stationery Office, London, 1948).
9. V. BUCUR and R. R. ARCHER, *Wood Sci. Technol.* **18** (1984) 255.
10. J. BODIG and B. A. JAYNE, "Mechanics of wood and wood composites" (Van Nostrand Reinhold, New York, 1982).
11. A. T. PRICE, *Phil. Trans. Roy. Soc.* A **228** (1928) 1.
12. M. F. ASHBY and L. J. GIBSON, *Proc. Roy. Soc. Lond.* A **382** (1982) 25.
13. W. W. BARKAS, *Trans. Faraday Soc.* **37** (1941) 535.
14. L. J. GIBSON, PhD thesis, University of Cambridge, (1981).
15. I. D. CAVE, *Wood Sci. Technol.* **2** (1968) 268.
16. J. M. DINWOODIE, "Timber, its nature and behaviour" (Van Nostrand Reinhold, New York, 1981).

Received 14 September 1992
and accepted 20 August 1993